

1 **MDA5 is critical to host defense during infection with**
2 **murine coronavirus**

3
4 **Zachary B. Zalinger, Ruth Elliott, Kristine M. Rose^{*}, and Susan R. Weiss[#]**

Department of Microbiology, Perelman School of Medicine, University of Pennsylvania,
Philadelphia, PA 19104-6076

Running title: MDA5 restricts MHV spread and pathogenesis

Key words: Murine coronavirus, MHV-induced hepatitis, MDA5 signaling

*Present address:

PATH
455 Massachusettes Ave, NW, suite 1000
Washington, DC 20001

#Corresponding author:

Susan R. Weiss
Department of Microbiology
University of Pennsylvania
Perelman School of Medicine
203A Johnson Pavilion
36th Street and Hamilton Walk
Philadelphia, PA 19104-6076
Phone: 215-898-8013
Email: weissr@upenn.edu

Abstract: 206 words

Text: 5,574 words

5

6

7 **ABSTRACT**

8 Infection with the murine coronavirus mouse hepatitis virus (MHV) activates the pattern
9 recognition receptors melanoma differentiation-associated gene 5 (MDA5) and toll-like
10 receptor 7 (TLR7) to induce transcription of type 1 interferon. Type 1 interferon is crucial for
11 control of viral replication and spread in the natural host, but the specific contributions of
12 MDA5 signaling to this pathway, as well as to pathogenesis and subsequent immune
13 responses, are largely unknown. In this study, we use MHV infection of the liver as a model
14 to demonstrate that MDA5 signaling is critically important for controlling MHV-induced
15 pathology and regulation of the immune response. Mice deficient in MDA5 expression
16 (MDA5^{-/-} mice) experienced more severe disease following MHV infection, with reduced
17 survival, increased spread of virus to additional sites of infection, and more extensive liver
18 damage. Although type 1 interferon transcription decreased in MDA5^{-/-} mice, the interferon
19 stimulated gene response remained intact. Cytokine production by innate and adaptive
20 immune cells was largely intact in MDA5^{-/-} mice, but perforin induction by natural killer cells,
21 and serum levels of interferon gamma, IL-6, and TNF α were elevated. These data suggest
22 that MDA5 signaling reduces the severity of MHV-induced disease, at least in part by
23 reducing the intensity of the pro-inflammatory cytokine response.

24

25

26

27

28

29

30

31 **IMPORTANCE**

32 Multicellular organisms employ a wide range of sensors to detect viruses and other
33 pathogens. One such sensor, MDA5, detects viral RNA and triggers induction of type 1
34 interferons, chemical messengers that induce inflammation and help regulate the immune
35 responses. In this study we sought to determine the role of MDA5 during infection with
36 mouse hepatitis virus, a murine coronavirus used to model viral hepatitis as well as other
37 human diseases. We found that mice lacking the MDA5 sensor were more susceptible to
38 infection and experienced decreased survival. Viral replication in the liver was similar in
39 mice with and without MDA5, but liver damage was increased in MDA5^{-/-} mice, suggesting
40 that the immune response is causing the damage. Production of several pro-inflammatory
41 cytokines was elevated in MDA5^{-/-} mice, suggesting that MDA5 may be responsible for
42 keeping pathological inflammatory responses in check.

43

44

45

46

47

48

49 **INTRODUCTION**

50 Eukaryotic cells use a variety of molecular sensors to detect pathogens, allowing
51 them to rapidly respond to infections. These sensors are called pattern recognition receptors
52 (PRRs), while the structures they detect are called pathogen associated molecular patterns
53 (PAMPs). The known critical PRRs for RNA viruses are the RIG-I-like receptors (RLR), RIG-
54 I and MDA5; non-RLR helicases such as DHX33 (1); and toll-like receptors (TLRs, in
55 particular TLR3, TLR7, and TLR8). Since these pathways are among the earliest host
56 responses triggered by infection, studying them is critically important for understanding
57 tropism, virulence, and regulation of host defense during viral infections.

58 RLRs are expressed in many cell types throughout the body and are therefore the
59 first sensors likely to detect many viral infections, regardless of route of entry or cellular
60 tropism. RIG-I and MDA5 detect different conformations of RNA, and not all RNA viruses
61 are detectable by both. Although first identified in the context of cancer (2, 3), MDA5 has
62 since been shown to have roles in host defense against a wide variety of viruses. MDA5 is
63 critical for type-1 interferon induction following coronavirus (4), picornavirus (5), and
64 influenza A (6) infection as well as for cytokine production in dendritic cells during norovirus
65 infection (7). Type 1 interferon constitutes an important component of the early innate
66 response by inducing a large number of interferon stimulated gene (ISGs) encoding antiviral
67 effectors. Type 1 interferon also plays a role in regulating the adaptive immune response in
68 that animals lacking MDA5 signaling ($MDA5^{-/-}$) demonstrate a variety of immunological
69 defects, including dysregulation of the adaptive immune response during West Nile virus (8)
70 and Theiler's virus infection (9).

71 The murine coronavirus mouse hepatitis virus (MHV) is a positive sense RNA virus of
72 Betacoronavirus lineage 2a. Laboratory strains of MHV have a diverse range of cellular and

73 organ tropisms, making them useful model organisms for studying host pathways involved
74 in tropism barriers and virulence (10). MHV strain A59 (MHV-A59) is dual tropic, infecting
75 primarily the liver and the central nervous system, causing moderate hepatitis and mild
76 encephalitis followed by chronic demyelinating disease (11). Intraperitoneal inoculation of
77 MHV-A59 leads to infection of the liver, spleen, and lungs in immunocompetent mice. MHV-
78 A59 can also replicate in the central nervous system when inoculated intracranially;
79 however, it cannot spread more than minimally from the periphery to the central nervous
80 system in immunocompetent mice. MHV-A59 causes hepatitis when it infects the liver and
81 acute encephalitis and chronic demyelination when it infects the central nervous system.
82 Other MHV strains infect the lung and gastrointestinal tracts, making MHV infection a model
83 for multiple human diseases (10, 12). The tropism and virulence of MHV infection are
84 partially determined by immunological factors, as infection of mice lacking type 1 interferon
85 signaling (*Ifnar1^{-/-}*) results in expanded organ tropism and greatly reduced survival (4, 13).
86 Although MDA5, but not RIG-I, is known to be necessary for induction of type I interferon in
87 cultured bone marrow derived macrophages (4) and microglia (data not shown), the
88 importance of MDA5 in induction of interferon during MHV infection has not been well
89 characterized.

90 Although type 1 interferon signaling is crucial for host defense against MHV and
91 MDA5 contributes to production of type 1 interferon in cell culture, it is unclear to what
92 extent MDA5 contributes to host defense during *in vivo* infections. In this study we found
93 that mice lacking MDA5 had similar levels of viral replication in the liver and spleen as wild
94 type C57BL/6 (WT) mice but were nevertheless more susceptible to infection, experiencing
95 decreased survival and increased hepatitis. Furthermore, the ISG response was intact,
96 suggesting a more complicated role for MDA5-induced interferon. Production of pro-

97 inflammatory cytokines was elevated in MDA5^{-/-} mice which, taken together with increased
98 hepatitis, suggests that MDA5 signaling limits the damage from pathological pro-
99 inflammatory immune responses.

100

101 **MATERIALS AND METHODS**

102 **Virus and mice**

103 Recombinant MHV strain A59 (referred to herein as MHV) has been described previously
104 (14, 15). The titer was determined by plaque assay on murine L2 cell monolayers, as
105 described previously (16). Wild type C57BL/6 (WT) mice were purchased from Jackson
106 Laboratories (Bar Harbor, ME). MDA5 deficient (MDA5^{-/-}) mice were a generous gift from
107 Dr. Michael S. Diamond (Washington University, St. Louis). Mice were genotyped and bred
108 in the animal facilities of the University of Pennsylvania. Four-to-six week old mice were
109 used for all experiments. For infections, virus was diluted in phosphate-buffered saline
110 (PBS) supplemented with 0.75% bovine serum albumin (BSA) and inoculated
111 intraperitoneally (i.p.). All experiments were approved by the University of Pennsylvania
112 Institutional Animal Care and Use Committee.

113

114 **Viral replication burden**

115 To monitor viral replication, mice were inoculated i.p. with 500 plaque-forming units (PFU) of
116 MHV and sacrificed 3, 5, and 7 days after infection. Following cardiac perfusion with
117 phosphate buffered saline, organs were harvested and placed in gel saline (an isotonic
118 saline solution containing 0.167% gelatin), weighed, and frozen at -80°C. Organs were later
119 homogenized, and plaque assays were performed on L2 fibroblast monolayers as
120 previously described (16).

121

122 Quantitative real time RT-PCR

123 Total RNA was purified from the lysates of homogenized livers using Trizol Reagent
124 (Invitrogen, Carlsbad, CA) according to the manufacturer's instructions. The resulting RNA
125 was treated with TURBO DNase (Ambion),. A custom Taqman Low Density Array (LDA)
126 was designed to include interferon stimulated gene probes (IRF-7, IRF-9, STAT1, STAT2,
127 ISG15, ISG56, IFN β , IFN α 4, RIG-I) and 2 control probes (18S and RPL13a). RNA (1 μ g)
128 was reverse-transcribed to cDNA using the High Capacity RNA-to-cDNA kit (Applied
129 Biosystems). The 384-well custom LDA plates were loaded with 50 μ L of cDNA and 50 μ L
130 of 2X Taqman Universal PCR Master Mix and run on a 7900 HT Blue instrument (Applied
131 Biosystems). The data were analyzed using SDS 2.3 software. The same genes were also
132 assayed by qRT-PCR as follows. RNA was reverse-transcribed using Superscript III reverse
133 transcriptase (Invitrogen) to produce cDNA, then amplified using primers obtained from
134 Integrated DNA Technologies (Coralville, IA). The sense and antisense primer sequences
135 are available upon request. Real time PCR was performed using iQ SYBR Green Supermix
136 (Biorad) on an iQ5 Multicolor Real-Time PCR detection system (Biorad). mRNA was
137 quantified as ΔC_T values relative to beta actin or 18S rRNA mRNA levels. ΔC_T values of
138 infected samples were expressed as fold changes over ΔC_T values of mock samples (\log_{10}).

139

140 Cell isolation from the spleen and liver

141 Wild type and MDA5 deficient (MDA5 $^{-/-}$) mice were infected i.p. with 500 PFU of MHV, and
142 organs were subsequently harvested after cardiac perfusion with PBS. Splenocytes were
143 rendered into single-cell suspensions through a 70-micron filter, after which red blood cells
144 were selectively lysed by incubating for 2 minutes in 0.206% tris HCl, 0.744% NH $_4$ Cl

145 solution. Livers were homogenized mechanically, then lysates were centrifuged through a
146 Percoll® gradient to obtain a single-cell suspension.

147

148 **Surface marker and intracellular cytokine staining**

149 Intracellular cytokine staining was performed on single cell suspensions of splenocytes
150 following a four-hour incubation with brefeldin A (20 µg/ml, Sigma) and the MHV peptides
151 M133 (MHC class II; 4 µg/ml, Biosynthesis) and S598 (MHC class I; 9.3 µg/ml,
152 Biosynthesis). T cells, natural killer and natural killer T cells were stained with the following
153 antibodies: CD3 (eBioscience, clone 17A2), CD4 (eBioscience, clone GK1.5), CD8
154 (eBioscience, clone 53-6.7), CD44 (eBioscience, clone IM7), CD11a (Biolegend, clone
155 M17/4), PD-1 (eBioscience, clone RMP1-30), βTCR (eBioscience, clone H57-597), γδTCR
156 (Biolegend, clone GL3), perforin (eBioscience, clone MAK-D), and interferon gamma
157 (eBioscience, clone XMG1.2). For innate cell immunophenotyping cells were stained with
158 the following antibodies: CD45 (Biolegend, clone 30-F11), Ly6G (Biolegend, clone 1A8),
159 Ly6C (Biolegend, clone HK1.4), CD11b (eBioscience, clone M1/70), CD11c (Biolegend,
160 clone N418), CD3 (Biolegend, clone 145-2C11), CD19 (BD, clone 1D3), and NK1.1
161 (eBioscience, clone PK136). For dendritic cell (DC) phenotyping experiments cells were
162 stained with the following antibodies: CD11b (eBioscience, clone M1/70), CD11c
163 (Biolegend, clone N418), CD3 (eBioscience, clone 17A2), CD19 (eBioscience, clone 1D3),
164 NK1.1 (eBioscience, clone PK136), CD45 (eBioscience, 30-F11), CD86 (Biolegend, clone
165 GL-1), CD80 (Molecular Probes, clone 16-10A1), MHC class II (eBioscience, clone
166 M5/114.15.2), B220 (Life Technologies, clone RA3-6B2), and PDCA-1/CD317 (eBioscience,
167 129c). Staining for interferon gamma was performed after permeabilization with
168 Cytofix/cytoperm Plus Fixation/Permeabilization kit (BD). Following staining, cells were

169 analyzed by flow cytometry on an LSR II (Becton Dickinson), and the resulting data were
170 analyzed using FlowJo software (Treestar).

171

172 **Liver histology**

173 Livers were harvested from sacrificed mice and fixed for 24 hours in 4% phosphate buffered
174 formalin, embedded in paraffin, and sectioned. Sections were stained with hematoxylin and
175 eosin. Four to five non-overlapping fields each 9×10^6 microns² in area were selected, the
176 number of inflammatory foci on each field was counted, and the mean was determined.
177 Samples in which foci had coalesced into a continuous confluence were scored as too
178 numerous to count (TNTC).

179

180 **T cell depletions**

181 Mice were inoculated with antibody i.p. two days prior to, and four and six days after,
182 infection with MHV. Mice received either a negative control antibody (LTF-2, Bio X Cell), or
183 a cocktail of a CD4 depleting antibody (GK1.5, Bio X Cell) and a CD8 depleting antibody
184 (2.43, Bio X Cell). All antibodies were at 250ug/ml concentration.

185

186 **RESULTS**

187 **MDA5^{-/-} mice are more susceptible to MHV infection.**

188 MHV-A59 is a dual tropic strain infecting primarily the liver and the central nervous system
189 of WT C57BL/6 mice. We (4) and others (13) have shown previously that mice lacking the
190 type 1 interferon receptor (*Ifnar1*^{-/-}) are acutely susceptible to MHV infection. Infection of
191 *Ifnar1*^{-/-} mice results in spread to multiple organs not usually infected in immunocompetent
192 mice and 100% lethality by day two post-infection. MHV has been shown to induce type 1

193 interferon via two pathways, MDA5 (4) and TLR7 (13) signaling. To determine whether mice
194 lacking MDA5 signaling were more or less vulnerable to infection with MHV, we infected
195 MDA5^{-/-} mice intraperitoneally (i.p.) with 500 PFU of dual tropic MHV, approximately one
196 tenth of a 50% lethal dose of this virus in wild type C57BL/6 mice. As expected, this dose
197 was nonlethal in all but a small minority of wild-type mice but lethal in roughly 75% of the
198 MDA5^{-/-} animals by 7 days post infection (Figure 1A).

199 Following i.p. inoculation, MHV replicates in the liver and several other organs of
200 C57BL/6 (WT) mice, with replication peaking at day 5 post-infection. Although capable of
201 replicating in the central nervous system, MHV does not readily cross the blood brain barrier
202 of most animals following i.p. inoculation of WT mice (1, 17). Inflammation and necrosis
203 peak in the liver at day 7 post infection (2, 18, 19). To determine if the absence of MDA5
204 expression results in increased viral replication relative to WT mice, we infected WT and
205 MDA5^{-/-} animals with 500 PFU of MHV. On days 3, 5, and 7 post infection animals were
206 sacrificed and their livers, spleens, brains, spinal cords, hearts, kidneys, and lungs were
207 assessed for viral replication by plaque assay. Mean viral titers in the liver and spleen were
208 similar between WT and MDA5^{-/-} mice (Figure 1B), suggesting that MDA5 is not required to
209 control the infection in those organs. However, in the absence of MDA5, increased viral
210 titers were observed in other organs. Replication was increased in the lungs, kidney, and
211 heart (Figure 1C), with a larger number of MDA5^{-/-} mice than WT mice having infection at
212 those sites (Figure 1C). Similarly, spread from the periphery to the central nervous system
213 was increased in MDA5^{-/-} mice (Figure 1B), suggesting that MDA5 signaling contributes to
214 the blood-brain barrier and other tropism barriers.

215 The severity of liver damage was compared between WT and MDA5^{-/-} mice by
216 hematoxylin and eosin staining of liver sections from mice sacrificed on days 3, 5, and 7

217 post-infection. The number of inflammatory foci in four to five non-overlapping fields of view,
218 each 9×10^6 microns², was counted and the mean number was determined. In some
219 samples the foci had combined to form a continuous confluence covering the entirety of the
220 section. These samples were scored as too numerous to count (TNTC). Despite the
221 similarity in viral replication in the liver between MDA5^{-/-} and WT mice, the prevalence of
222 inflammatory foci was higher in MDA5^{-/-} mice (Figure 2A). The increased severity of liver
223 damage despite unchanged viral replication in MDA5^{-/-} mice compared to WT mice suggests
224 that an immunopathological mechanism may underlie the greater susceptibility of MDA5^{-/-}
225 mice to MHV infection.

226

227 **The mRNA expression of type 1 interferon, but not interferon-stimulated genes, is**
228 **reduced in MDA5^{-/-} mice.**

229 The primary role of MDA5 is to upregulate type 1 interferon expression in response to viral
230 dsRNA. We hypothesized that mice lacking MDA5 would express less interferon, which
231 should in turn limit the activation of transcription of interferon-stimulated genes (ISGs). To
232 test this hypothesis we isolated RNA from the livers of infected WT and MDA5^{-/-} mice
233 collected 3, 5 and 7 days post infection and performed quantitative reverse transcription
234 PCR (qRT-PCR). Induction of interferon- β and $-\alpha 4$ mRNA expression in the livers of
235 infected mice relative to mock infected mice was lower for MDA5^{-/-} mice than for WT mice
236 on days 3 and 5 after infection, although this difference was transient, and was no longer
237 evident by day 7 post-infection (Figure 3A). We hypothesized that a biologically relevant
238 decrease in interferon expression would have downstream effects, most notably on
239 induction of anti-viral ISG expression, which could lead to the observed disease phenotype,
240 and therefore performed qRT-PCR to measure the expression of a representative panel of

241 ISGs in the liver. Surprisingly, ISG expression in MDA5^{-/-} mice was intact for almost all
242 genes at almost all time points despite the reduced induction of type I interferon mRNA
243 (Figure 3B). These results suggest that if the increased susceptibility of MDA5^{-/-} mice to
244 MHV infection is due to decreased interferon expression, it is not a result of reduced ISG
245 expression.

246

247 **Innate inflammatory cell recruitment is largely intact in MDA5^{-/-} mice, but activation of**
248 **dendritic cells is elevated.**

249 Shortly after infection, a diverse set of innate inflammatory cells infiltrate the sites of viral
250 replication, where they are often instrumental in restricting infection, regulating the adaptive
251 immune response, and causing immunopathology. We hypothesized that the loss of MDA5
252 signaling might cause dysregulation of the inflammatory infiltrate. A delay or reduction in
253 magnitude of the recruitment could allow the virus to replicate to higher levels or in different
254 organs or cell types, while over-exuberant recruitment could lead to tissue damage, as
255 observed in the livers of MDA5^{-/-} mice (Figure 2).

256 To determine if there were differences in the kinetics or magnitude of recruitment we
257 isolated and immunophenotyped cells from the livers of infected mice shortly after i.p.
258 inoculation with 500 pfu of MHV (Figure 4A). We observed no differences in the kinetics or
259 magnitude of recruitment of macrophages (CD3⁻CD19⁻NK1.1⁻CD45⁺Ly6-C⁻Ly6-G⁻CD11c⁻
260 CD11b⁺F4/80⁺), dendritic cells (CD3⁻CD19⁻NK1.1⁻CD45⁺Ly6-C⁻Ly6-G⁻CD11c⁺),
261 plasmacytoid dendritic cells (CD3⁻CD19⁻NK1.1⁻CD45⁺Ly6-C⁻Ly6-G⁻CD11c⁺B220⁺PDCA-1⁺),
262 neutrophils (CD3⁻CD19⁻NK1.1⁻CD45⁺Ly6-C⁻Ly6-G⁺), natural killer cells (CD3⁻CD19⁻
263 NK1.1⁺CD45⁺Ly6-C⁻Ly6-G⁻), or inflammatory monocytes (CD3⁻CD19⁻NK1.1⁻

264 CD45⁺CD11b⁺Ly6-C⁺Ly6-G⁻), indicating that early infiltration is largely independent of MDA5
265 signaling.

266 We also assessed the activation phenotype of plasmacytoid, lymphoid, and myeloid
267 dendritic cells (DCs). CD80 and CD86, co-activation markers utilized by DCs during T cell
268 priming (20, 21), are used as a marker of activation. Plasmacytoid DCs (pDCs) are a major
269 producer of type 1 interferon during MHV infection that rely on TLR7 rather than MDA5 to
270 detect MHV (3, 13). pDC-dependent type 1 interferon production should be intact in MDA5^{-/-}
271 mice, which may account for the intact ISG response. The co-expression of CD80 and
272 CD86 on pDCs was compared between MDA5^{-/-} and wild-type mice. The number of
273 CD80⁺CD86⁺ pDCs was lower on day 1, equal on day 2, and higher on day 3 post infection
274 in the MDA5^{-/-} mice (Figure 4B). We speculate that the larger number of activated
275 plasmacytoid dendritic cells at later time points may lead to higher production of interferon
276 driving expression of ISGs even in the absence of MDA5-dependent interferon. However,
277 TLR7-dependent interferon may also account for the interferon present in MDA5^{-/-} mice,
278 independent of pDC activation.

279 Lymphoid and myeloid DCs are involved in T cell priming. The co-expression of
280 CD80 and CD86 was higher on these populations in MDA5^{-/-} mice compared to WT mice
281 (Figure 4B). This may suggest that T cell priming is more robust in MDA5^{-/-} animals.

282 Although the magnitude and kinetics of natural killer cell infiltration into the liver was
283 independent of MDA5 signaling (Figure 4A), the function of these cells, as well as that of the
284 related natural killer T cells, is dependent on their production of interferon gamma and
285 perforin, and an MDA5-dependent defect in cytokine production could alter their efficacy
286 without affecting the size of the populations. To test whether cytokine production in either
287 cell population was dependent on MDA5 signaling we isolated cells from the spleen and

288 liver five days after infection and assessed their cytokine production by intracellular staining
289 and flow cytometry (Figure 5). The percent of each population producing interferon gamma
290 or perforin was similar between genotypes, with the exception of natural killer cells isolated
291 from the spleen, which exhibited elevated perforin production in mice lacking MDA5
292 signaling. Perforin is a driver of harmful pathology in many contexts (22-25), and may be in
293 the context of MHV infection as well. Elevated perforin production could lead to either the
294 increased liver damage, decreased survival, or both.

295

296 **Effect of MDA5 on the T cell response.**

297 A functional T cell response is essential for clearance of MHV infection. Both CD4
298 and CD8 T cells, as well as perforin and granzyme and the pro-inflammatory cytokine
299 interferon gamma, have been established to be necessary (4, 26). B cells appear to be
300 relevant only during a later stage of acute infection, at a time point after we see death
301 among MDA5^{-/-} mice (27, 28). Given that MDA5 can in some contexts be important for
302 regulating the T cell response (5, 8, 9) and that dendritic cells express higher levels of the
303 co-activating receptors CD80 and CD86 in MDA5^{-/-} mice, we hypothesized that CD4 and/or
304 CD8 T cells are dysregulated in MDA5^{-/-} animals. This could result in either a less effective
305 T cell response that is unable to control the virus or an over-exuberant T cell response that
306 produces pathology. To determine whether the T cell response was intact we compared the
307 activation states of CD4 and CD8 T cell populations isolated from the spleens of WT and
308 MDA5^{-/-} mice 7 days post infection. Isolated cells were stimulated with the M133 (class II)
309 and S598 (class I) MHV encoded peptides, which are the immunodominant class I and II
310 peptides during MHV infection (29, 30). Following stimulation the presence of the surface
311 activation markers CD44 and CD11a were analyzed by flow cytometry. The CD4 and CD8 T

312 cell populations from the spleens of MDA5^{-/-} animals were similar to those from WT mice in
313 terms of both the percentage of cells positive for each activation marker (Figure 6A) as well
314 as the total number of cells positive for each (Figure 6B). Statistically significant differences
315 between the genotypes are present in mock samples. However, these are minimal and we
316 believe them to have no biological significance.

317 We also found that CD11a⁺ CD4, CD44⁺ CD4, and CD11a⁺ CD8 T cells from MDA5^{-/-}
318 mice displayed a higher mean fluorescence intensity (MFI) of PD-1 staining (Figure 6C and
319 6D). While PD-1 is a marker of functionally defective, exhausted T cells during chronic
320 infection (9, 31), its role in acute infections remains unclear, with it marking both more and
321 less functional T cells, depending on the infectious context (32). The observation of more
322 severe liver pathology despite comparable viral replication in MDA5^{-/-} mice suggests that
323 PD-1 could be a marker of pathologically overactive T cells during MHV infection. However,
324 a less functional T cell response that is incapable of controlling viral replication could also
325 explain the increased viral spread and decreased survival, so PD-1 may instead be a
326 marker of less activated T cells in this context.

327 Cytokine production is a major effector function of both CD4 and CD8 T cells.
328 Reduced cytokine production in T cells from MDA5^{-/-} mice could suggest that the adaptive
329 immune response is too weak to control virus, while elevated cytokine levels could suggest
330 a damaging, pathological T cell response. Production of both interferon gamma and perforin
331 was assessed. Perforin production from CD8 T cells in both the spleen and liver was similar
332 in WT and MDA5^{-/-}, indicating that perforin production by T cells is independent of MDA5
333 signaling (Figure 7B). Production of interferon gamma was also similar between the
334 genotypes in both CD4 and CD8 T cells in the spleen (Figure 7C). However, a larger
335 proportion of CD4 and CD8 T cells from the livers of MDA5^{-/-} animals expressed interferon

336 gamma (Figure 7D). Since viral replication is similar in the liver between genotypes, this
337 may suggest that the adaptive immune response is over exuberant and may be
338 pathological.

339

340 **Mice depleted of T cells are more susceptible to MHV infection.**

341 To test the hypothesis that T cells are pathological in the absence of MDA5 signaling, we
342 depleted infected WT and MDA5^{-/-} mice of CD4 and CD8 T cells by administering a cocktail
343 of two depleting antibodies 2 days prior to and 4 and 6 days after infection. While we
344 expected to observe improved survival in mice without T cells, mice depleted of both CD4
345 and CD8 T cells had reduced survival compared to those mice given a control antibody
346 (Figure 8A). This suggests that either T cells are not pathological, or their pathological role
347 is outweighed by their antiviral role. Regardless, the poor survival of mice lacking MDA5
348 signaling is likely caused by a factor independent of the T cell response.

349

350 **Pro-inflammatory cytokines are elevated in the serum of MDA5^{-/-} mice.**

351 As T cells do not appear to be the cause of the low survival of MDA5^{-/-} mice, we considered
352 other drivers of inflammation. Pro-inflammatory cytokines, such as IL-6 and TNF α , are
353 produced early during infection by a variety of cell types. These cytokines can contribute to
354 control of pathogens, both before and after development of the adaptive immune response,
355 as well as drive damaging pathological responses. Inflammatory cytokines in the serum of
356 WT and MDA5^{-/-} mice were assayed to determine if levels were altered in the absence of
357 MDA5 signaling. Levels of interferon gamma, IL-6, and TNF α were all elevated in MDA5^{-/-}
358 mice as early as five days after infection (Figure 8B). This potent response may be the
359 causative agent of both increased pathology and decreased survival in MDA5^{-/-} mice,

360 suggesting that MDA5 has a regulatory role, inhibiting excessively strong pro-inflammatory
361 cytokine (Figure 8B) and perforin-mediated cellular (Figure 5) responses in order to protect
362 the host.

363

364 **DISCUSSION**

365 Induction of type 1 interferon expression is an early host response to viral invasion. In
366 the case of some viral models, including MHV infection of its natural host, type I interferon
367 signaling is vital to host survival (4, 10, 11, 13, 33). Alpha and beta interferon activate the
368 type 1 interferon receptor in an autocrine and paracrine manner to induce the expression of
369 ISGs. This set of genes includes additional type 1 interferon subtypes, various pro-
370 inflammatory cytokines and chemokines, MDA5 itself, and many other effectors (13, 34).
371 Through these ISGs, type 1 interferon constitutes a key component of the innate immune
372 response. In addition, interferon is often involved in regulating adaptive immune responses:
373 it can facilitate antigen presentation (35), promote clonal expansion among activated T cells
374 (36, 37), and enhance humoral responses (16, 38).

375 Type 1 interferon expression can be induced through numerous signaling pathways,
376 including RLR and TLR signaling. The interplay of these different pathways and the extent
377 to which they are redundant vary by context. We aimed to study the role of MDA5 signaling
378 specifically during MHV infection. Both MDA5 and TLR7 detect MHV infection, and mice
379 lacking TLR7 but not MDA5 are more susceptible to infection than wild-type mice but more
380 resistant than *Ifnar*^{-/-} mice (13), consistent with our findings here that interferon induced by
381 MDA5 signaling contributes to host protection.

382 We show here that MDA5^{-/-} mice are highly susceptible to MHV infection, with the
383 majority of MDA5^{-/-} animals dying by 7–8 days post infection while roughly 90% of WT

384 animals survived. Following i.p. inoculation viral replication levels in the liver and spleen
385 were similar between the genotypes, but virus more readily infected additional sites,
386 including the central nervous system, in MDA5^{-/-} mice, demonstrating a role of MDA5
387 signaling in maintaining organ tropism barriers. Despite similar levels of replication,
388 inflammation and pathology in the liver were more severe in the absence of MDA5 signaling.

389 We compared the host immune response to MHV between WT and MDA5^{-/-} mice and
390 found that many facets of the immune response were largely unchanged in the absence of
391 MDA5 expression. While induction of type 1 interferon expression is reduced in the livers of
392 MDA5^{-/-} mice, the ISG response was largely intact. The magnitude and kinetics of the innate
393 cellular infiltration of the liver were similar, as was the activation and cytokine production of
394 the T cell response in the spleen. This suggests that, unsurprisingly, many aspects of the
395 immune response are independent of type 1 interferon signaling.

396 Despite decreased levels of IFN β and IFN α 4 in MDA5^{-/-} mice relative to WT (Figure
397 3A), transcriptional induction of almost all tested ISGs was similar between the genotypes.
398 This demonstrates that interferon induced by TLR7 is sufficient to maintain ISG induction
399 even in the absence of MDA5 signaling, highlighting the redundancy within the interferon
400 response. However, despite this redundancy in ISG induction, MDA5^{-/-} mice still succumbed
401 rapidly to infection, suggesting that other downstream effects of MDA5 signaling are
402 necessary for full protection of the host. In addition, these observations indicate that some
403 downstream effects of type I interferon signaling were more susceptible to the loss of
404 MDA5-dependent interferon than others.

405 The dependence of organ tropism on route of inoculation makes MHV infection a
406 useful model for studying tropism barriers during viral infection. There is extensive literature
407 demonstrating that type 1 interferons play an important role in viral tropism (39). However,

408 infection studies in mice genetically deficient in interferon signaling components are often
409 confounded by the difficulty of distinguishing between tropism changes caused by disruption
410 of barriers and tropism changes caused by increased virus replication at primary sites of
411 infection leading to spillover into other organs. MDA5^{-/-} mice infected with MHV lack that
412 confounding factor because viral replication in the liver and spleen is unchanged. MHV
413 inoculated intracranially replicates in the central nervous system as well as in the liver,
414 spleen and lungs. However, when inoculated i.p. it does not readily cross the blood-brain
415 barrier and remains restricted to the liver, spleen and lungs in most infected mice. We have
416 shown that in MDA5^{-/-} mice, MHV was able to expand its tropism despite similar titers in the
417 primary sites of replication, frequently crossing the blood-brain barrier to infect the CNS after
418 i.p. inoculation and also spreading into and replicating in the heart and kidneys. This
419 demonstrates that the blood brain barrier and other tropism barriers depend in part on
420 MDA5 signaling. The effect of increased tropism during infection of MDA5^{-/-} mice remains to
421 be elucidated, but we hypothesize that it may lead to increased pathogenesis, and may
422 account for the increased virulence observed in mice lacking MDA5. Pathology in organs
423 that are infected at higher rates in MDA5^{-/-} mice than in WT mice may lead to death.

424 Lethality and liver damage were substantially higher in MDA5^{-/-} than WT mice, but,
425 surprisingly, there was not a corresponding difference in viral replication in the liver. This is
426 notably different from previous studies from our lab in which we compared hepatitis induced
427 by several strains of MHV and found an association between pathology and viral replication
428 in the liver in WT mice (18, 19). Since the increased pathology in the livers of MDA5^{-/-} mice
429 is not associated with a higher viral load in comparison with WT mice, we hypothesize that
430 the liver damage, and possibly the lethality, observed in MDA5^{-/-} mice is
431 immunopathological in nature. A similar phenomenon, in which effector functions normally

432 used to clear pathogens also damage host sites, leading to often severe pathology, has
433 been reported during infection with many other pathogens, including hepatitis B and C
434 viruses (40), Dengue virus (41), and *Toxoplasma gondii* (42). MDA5^{-/-} mice infected with
435 Theiler's virus generated higher levels of IL-17 and interferon gamma, both of which can
436 contribute to pathology (9). Taken in this context, our data suggest MDA5 may be important
437 for negative regulation of immune responses.

438 We had expected to observe a difference in the T cell response between MDA5^{-/-} and
439 WT mice due to the elevated expression of activation markers on dendritic cells. However,
440 by many metrics, including expression of activation markers, perforin expression, and
441 interferon gamma expression from cells in the spleen, the T cell response was similar
442 between genotypes. A similar observation was made during West Nile Virus infection, in
443 which the T cell response was also seemingly independent of MDA5 signaling (8). This
444 suggests that despite elevated expression of co-activation markers by DCs priming was
445 largely unchanged, although elevated production of interferon gamma by T cells in the liver
446 was observed, and may be a direct result of improved priming.

447 We found that T cells from MDA5^{-/-} mice had elevated expression of PD-1. PD-1/PD-
448 L1 signaling is a driver of T cell exhaustion during chronic infections (31), but its role during
449 acute infections is less clear. PD-1 expression correlated with a defective T cell response
450 during West Nile virus infection (8), and PD-1 signaling was found to weaken T cell
451 responses during acute infection with *Histoplasma capsulatum* (43) and rabies virus (44),
452 suggesting that PD-1 has similar roles in acute and chronic infections. However, PD-1/PD-
453 L1 signaling was shown to improve T cell responses during acute infection with *Listeria*
454 *monocytogenes* (45) and influenza (46), indicating that it can positively regulate T cells in
455 the context of some infections. We hypothesize that during MHV infection PD-1 expression

456 indicates strong activation of T cells and that these T cells induce pathology in the liver,
457 possibly accounting for the increased pathology. Jin *et al.* similarly found higher PD-1
458 ligand, PD-L1, expression on dendritic cells during Theiler's virus infection of MDA5^{-/-} mice,
459 as well as increased pathology and elevated levels of interferon gamma and IL-17 (9), both
460 of which can be drivers of pathology. We see no IL-17 production by T cells (data not
461 shown), and minimal changes in production of interferon gamma, so we speculate that while
462 the absence of MDA5 leads to immunopathology during both MHV and Theiler's virus
463 infection, the mechanism of pathology is different for each virus.

464 Survival of MDA5^{-/-} mice depleted of T cells was lower than those with T cells (Figure
465 8A), indicating that if the susceptibility of these mice to MHV infection is due to a lethal
466 immunopathological response, it is not driven by T cells. We do however observe elevated
467 expression of perforin by natural killer cells (Figure 5), and increased levels of the pro-
468 inflammatory cytokines interferon gamma, IL-6, and TNF α in the serum (Figure 8B) of
469 MDA5^{-/-} mice. We speculate that the low survival of MDA5^{-/-} mice is due to an
470 immunopathological response driven by one or more of these factors. These findings
471 suggest a context-dependent role for MDA5 as a negative regulator of the immune
472 response that limits immunopathology.

473

474

475

476 **ACKNOWLEDGMENTS.** This work was supported NIH grant R01-AI-060021 and NS-
477 054695 to S.R.W. Z.B.Z. was supported in part by training grant T32-NS007180. K.M.R.
478 was supported by T32-AI007324 and a diversity supplement to grant NS-054695.

479 Thanks to Drs. Helen Lazear and Michael S. Diamond, Washington University, St Louis, for
480 MDA5^{-/-} mice and help at early stages of the project.

481

482

483 **References**

484

- 485 1. **Mitoma H, Hanabuchi S, Kim T, Bao M, Zhang Z, Sugimoto N, Liu Y-J.** 2013. The
486 DHX33 RNA Helicase Senses Cytosolic RNA and Activates the NLRP3
487 Inflammasome. *Immunity* **39**:123–135.
- 488 2. **Kang D-C, Gopalkrishnan RV, Lin L, Randolph A, Valerie K, Pestka S, Fisher PB.**
489 2004. Expression analysis and genomic characterization of human melanoma
490 differentiation associated gene-5, mda-5: a novel type I interferon-responsive
491 apoptosis-inducing gene. *Oncogene* **23**:1789–1800.
- 492 3. **Kang D-C, Gopalkrishnan RV, Wu Q, Jankowsky E, Pyle AM, Fisher PB.** 2002.
493 mda-5: An interferon-inducible putative RNA helicase with double-stranded RNA-
494 dependent ATPase activity and melanoma growth-suppressive properties. *Proc. Natl.*
495 *Acad. Sci. U.S.A.* **99**:637–642.
- 496 4. **Roth-Cross JK, Bender SJ, Weiss SR.** 2008. Murine Coronavirus Mouse Hepatitis
497 Virus Is Recognized by MDA5 and Induces Type I Interferon in Brain
498 Macrophages/Microglia. *Journal of Virology* **82**:9829–9838.
- 499 5. **Kato H, Takeuchi O, Sato S, Yoneyama M, Yamamoto M, Matsui K, Uematsu S,**
500 **Jung A, Kawai T, Ishii KJ, Yamaguchi O, Otsu K, Tsujimura T, Koh C-S, Reis e**
501 **Sousa C, Matsuura Y, Fujita T, Akira S.** 2006. Differential roles of MDA5 and RIG-I
502 helicases in the recognition of RNA viruses. *Nature* **441**:101–105.

- 503 6. **Sirén J, Imaizumi T, Sarkar D, Pietilä T, Noah DL, Lin R, Hiscott J, Krug RM,**
504 **Fisher PB, Julkunen I, Matikainen S.** 2006. Retinoic acid inducible gene-I and mda-
505 5 are involved in influenza A virus-induced expression of antiviral cytokines. *Microbes*
506 *Infect.* **8**:2013–2020.
- 507 7. **McCartney SA, Thackray LB, Gitlin L, Gilfillan S, Virgin HW, Virgin Iv HW,**
508 **Colonna M.** 2008. MDA-5 recognition of a murine norovirus. *PLoS Pathog*
509 **4**:e1000108.
- 510 8. **Lazear HM, Pinto AK, Ramos HJ, Vick SC, Shrestha B, Suthar MS, Gale M,**
511 **Diamond MS.** 2013. Pattern Recognition Receptor MDA5 Modulates CD8+ T Cell-
512 Dependent Clearance of West Nile Virus from the Central Nervous System. *Journal of*
513 *Virology* **87**:11401–11415.
- 514 9. **Jin YH, Kim SJ, So EY, Meng L, Colonna M, Kim BS.** 2012. Melanoma
515 Differentiation-Associated Gene 5 Is Critical for Protection against Theiler's Virus-
516 Induced Demyelinating Disease. *Journal of Virology* **86**:1531–1543.
- 517 10. **Weiss SR, Leibowitz JL.** 2011. Coronavirus Pathogenesis, pp. 85–164. *In Advances*
518 *in Virus Research.* Elsevier.
- 519 11. **Lavi E, Gilden DH, Wroblewska Z, Rorke LB, Weiss SR.** 1984. Experimental
520 demyelination produced by the A59 strain of mouse hepatitis virus. *Neurology*
521 **34**:597–603.
- 522 12. **Bender SJ, Phillips JM, Scott EP, Weiss SR.** 2010. Murine Coronavirus Receptors
523 Are Differentially Expressed in the Central Nervous System and Play Virus Strain-
524 Dependent Roles in Neuronal Spread. *Journal of Virology* **84**:11030–11044.
- 525 13. **Cervantes-Barragan L, Züst R, Weber F, Spiegel M, Lang KS, Akira S, Thiel V,**
526 **Ludewig B.** 2007. Control of coronavirus infection through plasmacytoid dendritic-

- 527 cell-derived type I interferon. *Blood* **109**:1131–1137.
- 528 14. **MacNamara KC, Chua MM, Nelson PT, Shen H, Weiss SR.** 2005. Increased
529 Epitope-Specific CD8+ T Cells Prevent Murine Coronavirus Spread to the Spinal Cord
530 and Subsequent Demyelination. *Journal of Virology* **79**:3370–3381.
- 531 15. **Phillips JJ, Chua MM, Lavi E, Weiss SR.** 1999. Pathogenesis of chimeric
532 MHV4/MHV-A59 recombinant viruses: the murine coronavirus spike protein is a major
533 determinant of neurovirulence. *Journal of Virology* **73**:7752–7760.
- 534 16. **Hingley ST, Gombold JL, Lavi E, Weiss SR.** 1994. MHV-A59 fusion mutants are
535 attenuated and display altered hepatotropism. *Virology* **200**:1–10.
- 536 17. **Lavi E, Gilden DH, Highkin MK, Weiss SR.** 1986. The organ tropism of mouse
537 hepatitis virus A59 in mice is dependent on dose and route of inoculation. *Lab. Anim.*
538 *Sci.* **36**:130–135.
- 539 18. **Navas S, Seo SH, Chua MM, Sarma JD, Lavi E, Hingley ST, Weiss SR.** 2001.
540 Murine Coronavirus Spike Protein Determines the Ability of the Virus To Replicate in
541 the Liver and Cause Hepatitis. *Journal of Virology* **75**:2452–2457.
- 542 19. **Navas S, Weiss SR.** 2003. Murine Coronavirus-Induced Hepatitis: JHM Genetic
543 Background Eliminates A59 Spike-Determined Hepatotropism. *Journal of Virology*
544 **77**:4972–4978.
- 545 20. **Rudd CE, Taylor A, Schneider H.** 2009. CD28 and CTLA-4 coreceptor expression
546 and signal transduction. *Immunol. Rev.* **229**:12–26.
- 547 21. **Ueda H, Howson JMM, Esposito L, Heward J, Snook H, Chamberlain G, Rainbow**
548 **DB, Hunter KMD, Smith AN, Di Genova G, Herr MH, Dahlman I, Payne F, Smyth**
549 **D, Lowe C, Twells RCJ, Howlett S, Healy B, Nutland S, Rance HE, Everett V,**
550 **Smink LJ, Lam AC, Cordell HJ, Walker NM, Bordin C, Hulme J, Motzo C, Cucca**

- 551 **F, Hess JF, Metzker ML, Rogers J, Gregory S, Allahabadia A, Nithiyanthan R,**
552 **Tuomilehto-Wolf E, Tuomilehto J, Bingley P, Gillespie KM, Undlien DE,**
553 **Rønningen KS, Guja C, Ionescu-Tîrgoviște C, Savage DA, Maxwell AP, Carson**
554 **DJ, Patterson CC, Franklyn JA, Clayton DG, Peterson LB, Wicker LS, Todd JA,**
555 **Gough SCL.** 2003. Association of the T-cell regulatory gene CTLA4 with susceptibility
556 to autoimmune disease. *Nature* **423**:506–511.
- 557 22. **Novais FO, Carvalho LP, Graff JW, Beiting DP, Ruthel G, Roos DS, Betts MR,**
558 **Goldschmidt MH, Wilson ME, de Oliveira CI, Scott P.** 2013. Cytotoxic T cells
559 mediate pathology and metastasis in cutaneous leishmaniasis. *PLoS Pathog*
560 **9**:e1003504.
- 561 23. **Gebhard JR, Perry CM, Harkins S, LANE T, Mena I, Asensio VC, Campbell IL,**
562 **Whitton JL.** 1998. Coxsackievirus B3-induced myocarditis: perforin exacerbates
563 disease, but plays no detectable role in virus clearance. *The American Journal of*
564 *Pathology* **153**:417–428.
- 565 24. **Amrani A, Verdaguer J, Anderson B, Utsugi T, Bou S, Santamaria P.** 1999.
566 Perforin-independent beta-cell destruction by diabetogenic CD8(+) T lymphocytes in
567 transgenic nonobese diabetic mice. *J. Clin. Invest.* **103**:1201–1209.
- 568 25. **Kägi D, Odermatt B, Seiler P, Zinkernagel RM, Mak TW, Hengartner H.** 1997.
569 Reduced incidence and delayed onset of diabetes in perforin-deficient nonobese
570 diabetic mice. *J. Exp. Med.* **186**:989–997.
- 571 26. **Bergmann CC, Lane TE, Stohlman SA.** 2006. Coronavirus infection of the central
572 nervous system: host–virus stand-off. *Nat Rev Micro* **4**:121–132.
- 573 27. **Lin MT, Hinton DR, Marten NW, Bergmann CC, Stohlman SA.** 1999. Antibody
574 prevents virus reactivation within the central nervous system. *J. Immunol.* **162**:7358–

- 575 7368.
- 576 28. **Ramakrishna C, Stohlman SA, Atkinson RD, Shlomchik MJ, Bergmann CC.**
577 2002. Mechanisms of central nervous system viral persistence: the critical role of
578 antibody and B cells. *J. Immunol.* **168**:1204–1211.
- 579 29. **Castro RF, Perlman S.** 1995. CD8+ T-cell epitopes within the surface glycoprotein of
580 a neurotropic coronavirus and correlation with pathogenicity. *Journal of Virology*
581 **69**:8127–8131.
- 582 30. **Xue S, Jaszewski A, Perlman S.** 1995. Identification of a CD4+ T cell epitope within
583 the M protein of a neurotropic coronavirus. *Virology* **208**:173–179.
- 584 31. **Barber DL, Wherry EJ, Masopust D, Zhu B, Allison JP, Sharpe AH, Freeman GJ,**
585 **Ahmed R.** 2005. Restoring function in exhausted CD8 T cells during chronic viral
586 infection. *Nature* **439**:682–687.
- 587 32. **Brown KE, Freeman GJ, Wherry EJ, Sharpe AH.** 2010. Role of PD-1 in regulating
588 acute infections. *Current Opinion in Immunology* **22**:397–401.
- 589 33. **Ireland DDC, Stohlman SA, Hinton DR, Atkinson R, Bergmann CC.** 2007. Type I
590 Interferons Are Essential in Controlling Neurotropic Coronavirus Infection Irrespective
591 of Functional CD8 T Cells. *Journal of Virology* **82**:300–310.
- 592 34. **Loo Y-M, Fornek J, Crochet N, Bajwa G, Perwitasari O, Martinez-Sobrido L, Akira**
593 **S, Gill MA, García-Sastre A, Katze MG, Gale M.** 2008. Distinct RIG-I and MDA5
594 signaling by RNA viruses in innate immunity. *Journal of Virology* **82**:335–345.
- 595 35. **Stark GR, Kerr IM, Williams BR, Silverman RH, Schreiber RD.** 1998. How cells
596 respond to interferons. *Annu. Rev. Biochem.* **67**:227–264.
- 597 36. **Curtsinger JM, Valenzuela JO, Agarwal P, Lins D, Mescher MF.** 2005. Type I IFNs
598 provide a third signal to CD8 T cells to stimulate clonal expansion and differentiation.

- 599 J. Immunol. **174**:4465–4469.
- 600 37. **Kolumam GA, Thomas S, Thompson LJ, Sprent J, Murali-Krishna K.** 2005. Type I
601 interferons act directly on CD8 T cells to allow clonal expansion and memory
602 formation in response to viral infection. *J. Exp. Med.* **202**:637–650.
- 603 38. **Le Bon A, Schiavoni G, D'Agostino G, Gresser I, Belardelli F, Tough DF.** 2001.
604 Type I interferons potently enhance humoral immunity and can promote isotype
605 switching by stimulating dendritic cells in vivo. *Immunity* **14**:461–470.
- 606 39. **McFadden G, Mohamed MR, Rahman MM, Bartee E.** 2009. Cytokine determinants
607 of viral tropism. *Nature Publishing Group* **9**:645–655.
- 608 40. **Zignego AL, Piluso A, Giannini C.** 2008. HBV and HCV chronic infection:
609 autoimmune manifestations and lymphoproliferation. *Autoimmun Rev* **8**:107–111.
- 610 41. **Kurane I, Ennis FE.** 1992. Immunity and immunopathology in dengue virus
611 infections. *Seminars in Immunology* **4**:121–127.
- 612 42. **Israelski DM, Araujo FG, Conley FK, Suzuki Y, Sharma S, Remington JS.** 1989.
613 Treatment with anti-L3T4 (CD4) monoclonal antibody reduces the inflammatory
614 response in toxoplasmic encephalitis. *J. Immunol.* **142**:954–958.
- 615 43. **Lázár-Molnár E, Gácsér A, Freeman GJ, Almo SC, Nathenson SG, Nosanchuk**
616 **JD.** 2008. The PD-1/PD-L costimulatory pathway critically affects host resistance to
617 the pathogenic fungus *Histoplasma capsulatum*. *Proceedings of the National*
618 *Academy of Sciences* **105**:2658–2663.
- 619 44. **Lafon M, Mégret F, Meuth SG, Simon O, Velandia Romero ML, Lafage M, Chen L,**
620 **Alexopoulou L, Flavell RA, Prehaud C, Wiendl H.** 2008. Detrimental contribution of
621 the immuno-inhibitor B7-H1 to rabies virus encephalitis. *J. Immunol.* **180**:7506–7515.
- 622 45. **Rowe JH, Johanns TM, Ertelt JM, Way SS.** 2008. PDL-1 blockade impedes T cell

- 623 expansion and protective immunity primed by attenuated *Listeria monocytogenes*. *J.*
624 *Immunol.* **180**:7553–7557.
- 625 46. **Talay O, Shen C-H, Chen L, Chen J.** 2009. B7-H1 (PD-L1) on T cells is required for
626 T-cell-mediated conditioning of dendritic cell maturation. *Proceedings of the National*
627 *Academy of Sciences* **106**:2741–2746.

628

629

630

631

632 **FIGURE LEGENDS.**

633 **Figure 1. MDA5^{-/-} mice have heightened susceptibility to MHV infection.** Survival was
634 monitored after i.p. inoculation of 500 PFU MHV. Results were statistically significant by the
635 Mantel-Cox test (A). Viral titers in the liver, spleen, brain and spinal cord were determined
636 by plaque assay three, five and seven days after i.p. inoculation with 500 pfu MHV (B) and
637 at five days post inoculation in the lungs, heart and kidney (C). For panels B and C,
638 statistical significance was determined by a two-part test using a conditional t-test and
639 proportion test. Bars represent the mean. Data for all panels were pooled from two
640 independent experiments.

641

642 **Figure 2. MDA5^{-/-} mice have increased pathology in the liver.** Three, five and seven
643 days post i.p. inoculation with 500 PFU MHV livers were removed, fixed, sectioned and
644 stained with hematoxylin and eosin. Four to five non-overlapping fields of view, each 9x10⁶
645 microns², were chosen at random and the number of inflammatory foci was determined and
646 the mean was calculated (A). Statistical significance was determined by a two-part test

647 using a conditional t-test and proportion test. Samples in which foci had coalesced into a
648 continuous confluence were scored as too numerous to count (TNTC). Representative fields
649 are shown in B. Scale bar is 500 microns. Data are from one experiment.

650

651 **Figure 3. Interferon, but not interferon stimulated gene, expression is reduced in**
652 **MDA5^{-/-} mice.** On days 3, 5, and 7 days post i.p. inoculation with 500 PFU MHV, RNA was
653 isolated from the liver. Gene expression for type I interferons (A) and ISGs (B) was
654 quantified by qRT-PCR and expressed as fold over expression from mock-infected mice.
655 Statistical significance was determined by an unpaired, two-tailed t test. Outliers were
656 eliminated by a ROUT test (Q=1%). Bars represent the mean. Data were pooled from two
657 independent experiments, with the exception of viperin mRNA quantification, which was
658 performed once.

659

660 **Figure 4. Innate inflammatory cell recruitment is largely intact in MDA5^{-/-} mice, but**
661 **activation of dendritic cells is elevated.** On days 1, 2, and 3 post i.p. inoculation with 500
662 PFU MHV, mice were sacrificed, organs harvested and single cell suspensions derived from
663 the liver (A) or spleen (B) and immunophenotyped by staining with cell type specific
664 antibodies and analysis by flow cytometry. The total number of macrophages (CD3⁻CD19⁻
665 NK1.1⁻CD45⁺Ly6-C⁻Ly6-G⁻CD11c⁻CD11b⁺F4/80⁺), neutrophils (CD3⁻CD19⁻NK1.1⁻CD45⁺Ly6-
666 C⁻Ly6-G⁺), natural killer cells (CD3⁻CD19⁻NK1.1⁺CD45⁺Ly6-C⁻Ly6-G⁻), inflammatory
667 monocytes (CD3⁻CD19⁻NK1.1⁻CD45⁺CD11b⁺Ly6-C⁺Ly6-G⁻), and total dendritic cells (CD3⁻
668 CD19⁻NK1.1⁻CD45⁺Ly6-C⁻Ly6-G⁻CD11c⁺) are shown, normalized by the mass of the tissue
669 (A). Surface expression of the activation markers CD80 and CD86 was assessed on splenic
670 plasmacytoid (CD3⁻CD19⁻NK1.1⁻CD45⁺CD11c⁺B220⁺PDCA-1⁺), lymphoid (CD3⁻CD19⁻

671 NK1.1⁻CD45⁺CD11c⁺CD11b⁻), and myeloid (CD3⁻CD19⁻NK1.1⁻CD45⁺CD11c⁺CD11b⁻)
672 dendritic cells, and total number of CD80⁺CD86⁺ DCs of each subtype is shown (B).
673 Statistical significance was determined by an unpaired, two-tailed t test. Bars represent the
674 mean. Data were pooled from two independent experiments.

675

676 **Figure 5. Cytokine production by natural killer and natural killer T cells is similar or**
677 **elevated in MDA5^{-/-} mice compared to WT mice.** WT and MDA5^{-/-} mice were sacrificed
678 five days after i.p. inoculation with 500 PFU MHV, spleens and livers were harvested and
679 single cell suspensions derived from the organs were incubated with brefeldin A for three
680 hours, and immunophenotyped by staining with cell type specific antibodies. Cells were
681 permeabilized and stained with antibody specific to interferon gamma and perforin, then
682 analyzed by flow cytometry. Natural killer (CD3⁻NK1.1⁺) and natural killer T cells
683 (CD3⁺NK1.1⁺) were assessed. Statistical significance was determined by an unpaired, two-
684 tailed t test. Bars represent the mean. Data were pooled from two independent experiments.

685

686 **Figure 6. T cell activation is independent of MDA5 signaling.** Day 7 post i.p. inoculation
687 with 500 PFU MHV, mice were sacrificed, spleens harvested and single cell suspensions
688 were derived from the spleens of wild type and MDA5^{-/-} mice. Cells were
689 immunophenotyped by staining with cell type specific antibodies and analysis by flow
690 cytometry. The percent (A) and total number (B) of CD4 (CD3⁺CD4⁺) and CD8 (CD3⁺CD8⁺)
691 T cells with elevated surface expression of CD44 and CD11a are shown. Expression of PD-
692 1 (representative image, C) was assessed on CD44⁺ and CD11a⁺ CD4 and CD8 T cells (D).
693 Statistical significance was determined by an unpaired, two-tailed t test. Bars represent the
694 mean. Data are representative of two independent experiments.

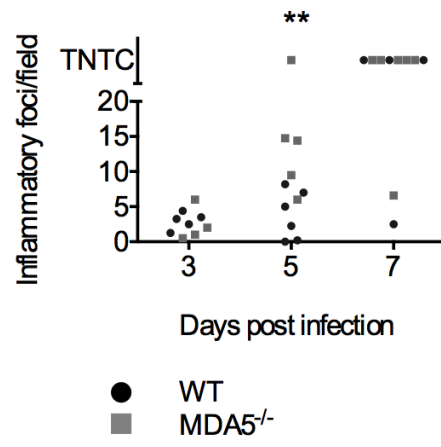
695

696 **Figure 7. Interferon gamma production, but not perforin production, is elevated in T**
697 **cells from MDA5^{-/-} mice.** WT and MDA5^{-/-} mice were sacrificed seven days after i.p.
698 inoculation with 500 PFU MHV, spleens and livers were harvested and single cell
699 suspensions derived from the organs were incubated with immunodominant MHV peptides
700 S598 (class I) and M133 (class II), and immunophenotyped by staining with cell type
701 specific antibodies. Cells were permeabilized and stained with antibody specific to interferon
702 gamma and perforin, then analyzed by flow cytometry (representative image, A). CD8
703 (CD3⁺CD8⁺) T cells, cells from the spleen and liver were assessed for expression of perforin
704 (B). CD4 (CD3⁺CD4⁺) and CD8 (CD3⁺CD8⁺) T cells from the spleen (C) and liver (D) were
705 also assessed for expression of interferon gamma. Statistical significance was determined
706 by an unpaired, two-tailed t test. Bars represent the mean. Data are representative of two
707 independent experiments.

708

709 **Figure 8. Elevated cytokines, but not T cells, may explain decreased survival of**
710 **infected MDA5^{-/-} mice.** MDA5^{-/-} mice were treated with CD4 and CD8 depleting antibodies
711 or a negative control -2, 4, and 6 days after infection with 500 PFU MHV inoculated i.p.
712 Survival was monitored (A). Data were pooled from two independent experiments. Results
713 are non-significant by the Mantel-Cox test. Serum was collected from WT and MDA5^{-/-} mice
714 with intact T cell compartments 3, 5, and 7 days after i.p. inoculation of 500 PFU MHV, and
715 analyzed for levels of interferon gamma, IL-6, and TNF α by ELISA (B). Statistical
716 significance was determined by a two-part test using a conditional t-test and proportion test.
717 Data were pooled from four independent experiments, n of 3-6.

718

A**B**